pISSN 0898-5901 | eISSN 1884-7269
Indexed in Scopus

Volume 29 - N. 3 - December 2022

Chitosan adhesives with sub-micron structures for photochemical tissue bonding

Samuel J. Frost,[1] Jessica Houang,[2] James M. Hook,[3] Antonio Lauto[2]

[1]The College, Western Sydney University, NSW; [2]School of Science, Western Sydney University, Penrith, NSW; [3]School of Chemistry, University of New South Wales, Sydney, NSW, Australia

ABSTRACT

We describe a method for fabricating biocompatible chitosan-based adhesives with sub-micron structures to enhance tissue bonding. This procedure avoids coating and chemical modification of structures and requires a simple drop-casting step for the adhesive film formation. Chitosan thin films (27±3 μm) were fabricated with sub-micron pillars (rectangular cuboid with height ~150 nm, square dimension ~1 μm and pitch ~2 μm) or holes (diameter ~500 nm or ~1 μm, depth ~100 or 400 nm, pitch of 1 or 2 μm). Polydimethylsiloxane moulds were used as negative templates for the adhesive solution that was cast and then allowed to dry to form thin films. These were applied on bisected rectangular strips of small sheep intestine and photochemically bonded by a green laser (λ= 532 nm, irradiance ~110 J/cm^2). The tissue repair was subsequently measured using a computer-interfaced tensiometer. The mould sub-micron structures were reproduced in the chitosan adhesive with high fidelity. The adhesive with pillars achieved the highest bonding strength (17.1±1.2 kPa) when compared to the adhesive with holes (13.0±1.3 kPa, $p<0.0001$, one-way ANOVA, n=15). The production of chitosan films with patterned pillars or holes in the sub-micron range was demonstrated, using a polydimethylsiloxane mould and a single drop-casting step. This technique is potentially scalable to produce adhesives of larger surface areas.

Key words: Nanostructures; nanofabrication; tissue repair; tissue engineering.

Running Head:
Chitosan adhesives with nanostructures for PTB
Corresponding author:
Antonio Lauto
Telephone: +61.2.46203235
Email: A.Lauto@westernsydney.edu.au

Introduction

Bioadhesives have long been explored as an alternative to sutures and staples for surgical applications.[1-3] While tissue bioadhesives are often used clinically in addition to conventional methodologies, they are still not considered as reliable due to less than adequate bonding strength where the tissue is under load.[4,5] With recent advances in nanotechnology, however, many new advanced bio-inspired adhesives have been fabricated, often drawing inspiration from the footpads of insects and small animals such as the cricket,[6] the beetle,[7] and the gecko.[8-11] These micro and nano- structured bioadhesives rely heavily on van der Waals forces to attach, but due to the wet physiological environment the forces are significantly weakened.[12] In order to overcome this problem, researchers have developed multi-stepped fabrication processes whereby the adhesive structures are coated or chemically modified in order to better facilitate adhesion.[13-15] Lana *et al.*, for example, used a silicon patch (polydimethylsiloxane or PDMS) for the treatment of tympanic membrane perforation.[16] The patch had micropillars coated with Dow Corning® MG 7-1010 Soft Skin Adhesive to enhance tissue attachment and the hearing function was immediately partially restored after patch application in mice. A multistep fabrication process is nonetheless technologically challenging, and a simpler technology is preferable. This issue was solved by the design and fabrication of a mono-layered nano-structured adhesive film based on chitosan and rose Bengal, which was reported by our group.[17] The adhesive did not require coating or chemical modification of nanostructures but was photochemically activated by green light, resulting in an adhesion strength of ~21 kPa when bonded to tissue. Despite this success, the fabrication of polycarbonate nanostructured moulds (necessary to obtain the adhesive) is technically demanding, costly and time consuming. In this investigation, PDMS moulds have instead been used to fabricate chitosan adhesives with sub-micron structures. These were not only easy to make but the surface topography of the moulds was also reproduced with high fidelity.

Materials and Methods

Mould Fabrication

The moulds for the nano-templates used in this investigation were fabricated at the University of Sydney Nano Institute (Sydney, Australia). In brief, a mask pattern is printed on a silicon photoresist using a combination of either photo-lithography or electron-beam lithography in the desired shape (for example 500 nm dots with a pitch of 1 μm). After the silicon template was fabricated, liquid PDMS was cast over the surface and cured. The PDMS layer was then removed and inverted, forming the reusable nano-structured mould (2 cm x 3 cm) that was employed in casting the chitosan adhesive.

Adhesive Fabrication

All chemicals were purchased from Sigma-Aldrich (Sydney, Australia) and were used without any further purification. An in-depth description of the adhesive preparation has previously been published.[18] Briefly, deacetylated chitosan (≥80%, MMW) was dissolved at a concentration of 1.7% w/v in deionised water (50 mL) containing acetic acid (2% w/v) and rose Bengal (RB, 0.01% w/v). The solution was stirred for 14 days at room temperature (25°C) and shielded from light to avoid photo-bleaching of the RB. The resultant solution was then centrifuged at 3270g for 1 hour to eliminate impurities. The supernatant was collected and stored in the refrigerator at 4°C prior to use. Using a sterile syringe, the rose adhesive solution was then spread evenly over the patterned section of the PDMS nano-structured template at a ratio of 2 mL to 12 cm^2, as previously reported.[17] After drop-casting, the adhesive was left on a level surface that was shielded from light to dry for ~3 weeks under clean conditions, atmospheric pressure, and a temperature of 25°C. The newly created nano-structured adhesive films were carefully removed from the templates with forceps and the thickness (27±3 μm) was measured with a digital micrometer (Model 293-831, Mitutoyo, Japan). The nano-structured films were then cut into strips of ~6×10 mm^2 and carefully stored in a flat plastic container shielded from light prior to use.

Group I

The mould (negative) consisted of a repeating regular square-shaped hole grid pattern. The holes had a depth of 150 nm, a width of 1 μm and a pitch (distance between the centre of one structure to the neighboring structure) of 2 μm. The resulting nano-adhesive replicated the inverse of this pattern with square-pillared structures instead of holes.

Group II

The mould consisted of regular-repeating round pillars with a height of 400 nm, width of 1 µm and pitch of 2 µm. In contrast to the adhesive produced in Group I, the nano-adhesive had holes matching the inverse of the template instead of pillars (~400 nm deep).

Group III

The mould template consisted of regular-repeating round pillars with a height of 100 nm, width of 500 nm and pitch of 1 µm. The pattern produced was very similar to the pattern used in Group II on a smaller scale. The nano-adhesive produced regular holes ~100 nm deep and 500 nm wide.

Photochemical Tissue Bonding

The nano-adhesives I, II, and III were tested in vitro on small sheep intestine. Tissue sections (~20×10 mm^2) were bisected and the adventitial layer was gently removed with scissors under an Olympus operating microscope. The intestine was kept moist using ~40 µL of water while the incision stumps were approximated end-to-end. Excess water was removed with cotton tips before a rose adhesive film (~6×10 mm^2) was positioned across the bisection line on the serosa layer with microforceps ensuring full contact with the intestine. Thereupon, a diode-pumped solid-state laser (CNI, Changchun 130103, China) serially spot-irradiated the strip, ensuring each spot was irradiated for ~5 seconds before moving the beam to the adjacent spot (λ=532 nm", spot size ~0.5 cm). The laser beam scanned the whole surface area of the adhesive several times in order to deliver ~110 J/cm^2.[19] During irradiation, the adhesive temperature remained below 39°C.[1,19] The laser was coupled to a multimode optical fibre (core diameter = 200 µm and numerical aperture = 0.22) that was inserted into a hand-held probe to provide easy and precise beam delivery. The laser parameters are summarized in Table 1.

Repair Strength

The repair strength of samples from groups I-III, both with and without irradiation (n=15 for each group), were tested with a calibrated single-column tensiometer (Instron 3343, Instron, MA, USA) that was interfaced with a personal computer. The tissue was kept moist in a sealed chamber before the tensile test to avoid sample desiccation. A sample was clamped to the tensiometer using mechanical grips that moved at a rate of 22 mm/min until the two tissue sections had separated. The maximum load at which the stumps separated (80% load drop) was recorded and the repair strength estimated by dividing the Max Load BY the surface area of the adhesive.[20]

Atomic Force Microscopy

The surface topography of the samples in each group were characterised using an atomic force microscope (AFM) (NanoWizard II, JPK Instruments AG, Germany). Five separate films from each group were mounted onto glass slides and scanned, with the surface roughness calculated over the scanned area (10 µm×10 µm). The AFM operated in intermittent contact mode in air using silicon cantilevers with a nominal spring constant of 36 N/m and a resonant frequency of 300 kHz (type ACT, AppNano, USA). The scanning rate was set to 1 Hz with a pixel resolution of 512×512.

Statistical Analysis

Data analysis was performed using an unpaired two-tailed t-test for simple group comparisons, or a one-way ANOVA with Tukey's multiple comparisons test. All tests were conducted at a confidence level of 95%. Values are reported as mean ± standard deviation.

Results

The adhesive that was drop-cast on the PDMS nano-structured templates replicated the inverse of the surface topography with high fidelity and minimal defects (Fig-

Table 1. Laser parameters for the photochemical bonding of the nano-structured adhesive to sheep small intestines.

Area (mm^2)	Power (mW)	Time (s)	Fluence (J/cm^2)	Irradiance (W/cm^2)	Spot Size (mm)
60 ± 5	180 ± 5	365 ± 5	110 ± 10	~0.9	~5

Area: surface area of the adhesive; Power: laser power (mean ± maximum error); Time: irradiation time (mean ± maximum error); Fluence: average laser fluence, Irradiance: estimated irradiance; Spot Size: size of the laser spot.

ures 1-3). The pillars present on the adhesive in Group I (Figure 1) had a height of ~150 nm and were square in shape with dimensions of ~1 µm and a pitch of ~2 µm. There were some minor defects present in ~15% of the square pillars that had a surface root mean square roughness (Rq) of ~36 nm (n=5). In contrast with the adhesive in Group I, the adhesives in Groups II and III had circular holes instead of square pillars. Group II (Figure 2) had holes of ~400 nm deep and ~1 µm in diameter with very minimal surface defects and an Rq of ~147 nm (n=5). Group III (Figure 3) had a much smaller hole-size with a depth of ~100 nm, diameter of ~500 nm and Rq of ~30 nm (n=5).

Laser Tissue Repair

The nano-structured adhesives from all three groups bonded successfully to tissue with and without treatment with the laser (Figure 4). The strongest of the three groups tested was the adhesive with pillars (Group I), having a bonding strength of 17.1±1.2 kPa with laser irradiation and 2.7±0.8 kPa without laser irradiation (n=15). These bonding strengths were significantly stronger than the nano-structured adhesives with holes in Groups II and III (p<0.0001, one-

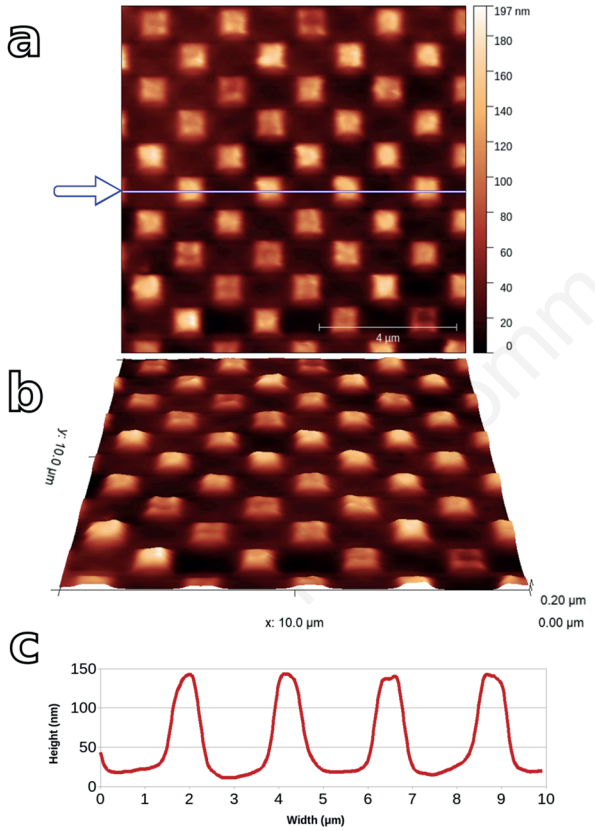

Figure 1. a) A two-dimensional AFM image showing a typical 10 × 10 µm area of the nano-structured rose adhesive from Group I. The pillars are ~1 µm wide and ~150 nm in height; b) A three-dimensional representation of the data shown in (a); c) A line scan showing a cross-section of the surface topography as denoted by the arrow in (a).

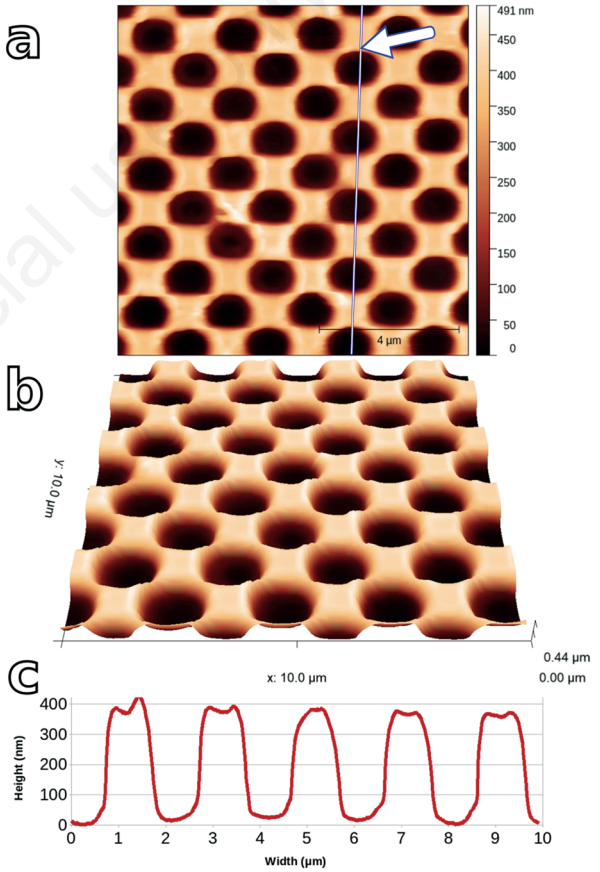

Figure 2. a) A two-dimensional AFM image showing a typical 10 × 10 µm area of the nano-structured rose adhesive from Group II. The holes are ~ 1 µm wide and ~400 nm deep; b) A three-dimensional representation of the data shown in (a). Unlike the adhesive in Group I, there are no peaks protruding from the surface. This leaves a much flatter adhesive with no observable defects; c) A line scan showing a cross-section of the surface topography as denoted by the arrow in (a).

way ANOVA, Tukey's multiple comparisons test). The adhesive with the smaller hole diameter (~500 nm) produced photochemical tissue bonds that were slightly stronger than the adhesive with 1 µm hole diameter (13.0±1.3 kPa and 11.4±0.7 kPa respectively, p=0.0006, one-way ANOVA, Tukey's multiple comparisons test). No significant difference in bonding strength was measured between these two groups without laser irradiation (0.7±0.3 kPa and 0.7±0.2 kPa respectively, p=0.9915, one-way ANOVA, Tukey's multiple comparisons test).

Discussion

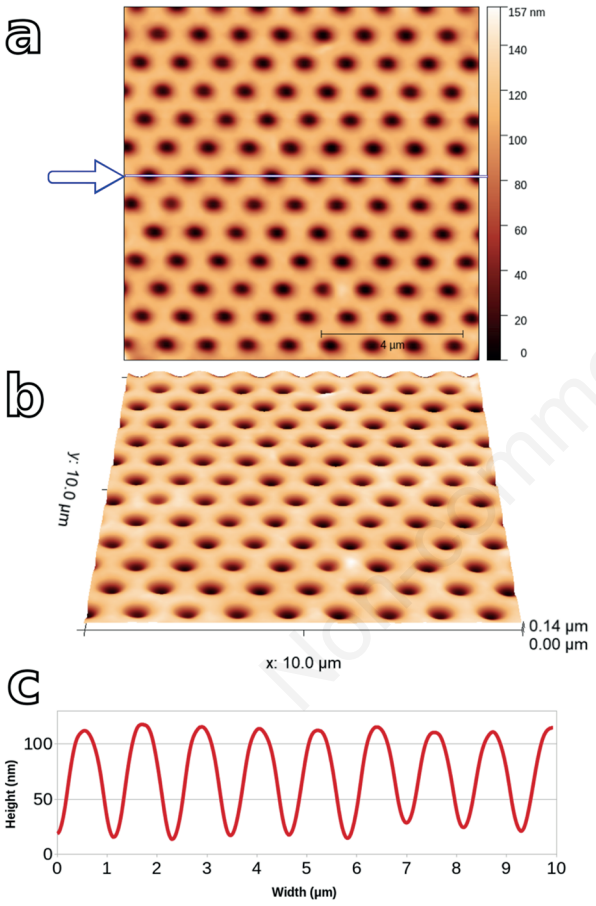

Figure 3. a) A two-dimensional AFM image showing a typical 10 × 10 µm area of the nano-structured rose adhesive from Group III. The holes are ~ 500 nm wide and ~ 130 nm deep; b) A three-dimensional representation of the data shown in (a). The surface topography is very similar to the adhesive in Group II but with smaller holes; c) A line scan showing a cross-section of the surface topography as denoted by the arrow in (a).

The development and fabrication of micro- and nano-structured adhesives has been underway for several years. It is only recently that these adhesives have been adapted to work under wet conditions such as those found in a physiological environment. The majority of these adhesives require a multi-step fabrication process whereby the interfacial structured surface is coated with a traditional adhesive or polymer to facilitate adhesion in a wet environment.[21,22] Lee *et al.* demonstrated this process by coating nano-structured PDMS pillars with a thin coating of poly(dopamine-co-methoxyethyl acrylate) (poly(DMA-co-MEA), resulting in strong reversible adhesion in a submerged environment.13 While capable of adhesion under wet conditions, this adhesive contains a non-biodegradable component (*i.e.*, PDMS). A more suitable adhesive was produced by Mahdavi *et al.* in which nano-structured adhesives (0.1–1 µm width and 0.8–3.0 µm height) were produced in a multi-step process, whereby

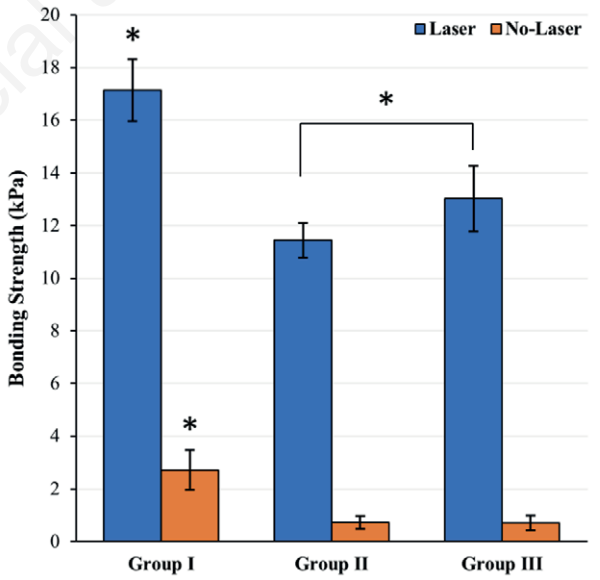

Figure 4. Bonding strength of the adhesives in Groups I, II, and III (n = 15 per group). The bonding strength of adhesives with pillars was significantly stronger than the adhesives with holes ($p < 0.0001$, one-way ANOVA). The adhesive with 500 nm holes (Group III) was also stronger than the adhesive with 1 μm holes (Group II, p=0.0006, one-way ANOVA). The bonding strength of adhesives with pillars (Group I) with no laser irradiation was also significantly stronger than that of adhesives with holes (Groups II and III, *$p < 0.0001$, one-way ANOVA) while there was no significant difference between the bonding strength of the adhesives in Groups II and III ($p = 0.9915$, one-way ANOVA).

poly(glycerol- co-sebacate acrylate) (PGSA) was coated with aldehyde functionalised dextran.[14] This resulted in a maximum separation force of 4.8 N/cm^2 when bonded to porcine small intestinal tissue in vitro. Microstructured films have also been produced from chitosan using PDMS templates resulting in pillar dimensions of ~1 µm in height and ~5 µm in width.[23] The films fabricated were not capable of tissue bonding and, in order to avoid dissolution in water, were washed several times with sodium hydroxide causing the films to swell upon contact with water. This swelling may impair the ability of reproducing film structures on the nanoscale. Recently, a much simpler process for developing nano-structured adhesives was demonstrated by our group, whereby the chitosan-based rose adhesive solution is plated on a polycarbonate mould and peeled off in one step, resulting in a bonding strength of ~21 kPa when irradiated with a green laser on sheep small intestine.[17] This method, while having produced a biocompatible and non-coated adhesive, still requires the fabrication of an elaborate polycarbonate nano-patterned mould. In this paper, we adopted a similar process using a simpler sub-micron mould instead for the adhesive fabrication. This PDMS mould resulted in few defects in the final adhesive even if they were reused multiple times. In fact, no observable change was noted in the topography of the sub-micron adhesive, as visualised by the AFM. The PDMS mould also provided an easier method of adhesive detachment after drying the chitosan-based solution. The silicon photoresist used to produce the PDMS moulds are re-usable, leading to the ability of producing adhesives on a larger scale (3x6 cm for example), hence cutting the cost, time, and complexity currently required by other methodologies. The bonding strength of the adhesives with sub-micron holes is weaker than previously reported values of ~15 kPa for the same rose adhesive without any micro or nanostructures.[1] We may hypothesize that this is due to the decreased area that is in contact with tissue in this type of adhesive. By calculating the ratio between the area of a circular hole with diameter, D, and a square with dimension, 3D, it is possible to estimate the effective adhesive surface in contact with tissue and thus estimate the bonding strength. In more detail,

$$\frac{\pi D^2}{4} * \frac{1}{9D^2} \sim 8.7\%$$

is the missing area in the adhesive of groups II and III. This fraction of adhesive surface is responsible for a loss in bonding strength of about 15 kPa x 8.7% = 1.3 kPa. Thus, an estimated bonding strength of 13.7 kPa is predicted for the group II and III adhesives. This value is close to the measured bonding strengths of Group II (11.4±0.7 KPa) and Group III (13.0±1.2 kPa) adhesives. From our preliminary analysis, it appears that photochemical bonding is primarily responsible for adhesion while other causes, such as capillary forces, are not. The bonding strength of the adhesive with holes may nevertheless perform better in *in vivo* animal models where tissue can grow through the holes and integrate with the adhesive, thereby stabilizing the repair site. Further studies are needed to test the performance of the proposed sub-micron adhesives *in vivo*.

Conflict of interest: The Authors declare no conflict of interest.

Availability of data and materials: All data generated or analyzed during this study are included in this published article.

Ethics approval and consent to participate: Not applicable.

Informed consent: Not applicable.

Conclusions

In this investigation, the production of chitosan films with patterned pillars or holes in the sub-micron range was demonstrated. These biocompatible films bond effectively to tissue upon irradiation with a green laser and are easily fabricated in a single drop-casting step with high fidelity from a pre-manufactured PDMS mould. This technique is potentially scalable to the production of adhesives with larger surface areas.

References

[1] Barton M, Morley JW, Stoodley MA, *et al.* Laser-activated adhesive films for sutureless median nerve anastomosis: laser-activated adhesive films. J Biophotonics 2013;6:938–49.
[2] Barton MJ, Morley JW, Stoodley MA, *et al.* Long term recovery of median nerve repair using laser-activated chitosan adhesive films: sutureless median nerve repair. J Biophotonics 2015;8:196–207.

[3] Sliow A, Ma Z, Gargiulo G, *et al*. Stimulation and Repair of Peripheral Nerves Using Bioadhesive Graft-Antenna. Adv Sci 2019;6:1801212.
[4] Shapiro AJ, Dinsmore RC, North JHJ. Tensile strength of wound closure with cyanoacrylate glue. Am Surg 2001;67:1113–5.
[5] Komatsu F, Mori R, Uchio Y. Optimum surgical suture material and methods to obtain high tensile strength at knots: problems of conventional knots and the reinforcement effect of adhesive agent. J Orthop Sci Off J Japanese Orthop Assoc 2006;11:70–4.
[6] Varenberg M, Gorb S. A beetle-inspired solution for underwater adhesion. J R Soc Interface 2008;5:383–5.
[7] Gorb SN. Biological attachment devices: exploring nature's diversity for biomimetics. Philos Trans R Soc A Math Phys Eng Sci 2008;366:1557–74.
[8] Autumn K, Liang YA, Hsieh ST, *et al*. Adhesive force of a single gecko foot-hair. Nature 2000;405:681–5.
[9] Rong Z, Zhou Y, Chen B, *et al*. Bio-inspired hierarchical polymer fiber-carbon nanotube adhesives. Adv Mater 2014;26:1456–61.
[10] Hu H, Wang D, Tian H, *et al*. Bioinspired hierarchical structures for contact-sensible adhesives. Adv Funct Mater 2022;32:2109076.
[11] Shi W, Cheng X, Cheng K. Gecko-inspired adhesives with asymmetrically tilting-oriented micropillars. Langmuir 2022;38:8890–8.
[12] Bergström L. Hamaker constants of inorganic materials. Adv Colloid Interface Sci 1997;70:125–69.
[13] Lee H, Lee BP, Messersmith PB. A reversible wet/dry adhesive inspired by mussels and geckos. Nature 2007;448:338–41.
[14] Mahdavi A, Ferreira L, Sundback C, *et al*. A biodegradable and biocompatible gecko-inspired tissue adhesive. Proc Natl Acad Sci 2008;105:2307–12.
[15] Pereira MJN, Sundback CA, Lang N, *et al*. Combined surface micropatterning and reactive chemistry maximizes tissue adhesion with minimal inflammation. Adv Healthc Mater 2014;3:565–71.
[16] Moreira Lana G, Sorg K, Wenzel GI, *et al*. Self-adhesive silicone microstructures for the treatment of tympanic membrane perforations. Adv NanoBiomed Res 2021;1: 2100057.
[17] Frost SJ, Mawad D, Higgins MJ, *et al*. Gecko-inspired chitosan adhesive for tissue repair. NPG Asia Mater 2016;8: e280.
[18] Lauto A, Stoodley M, Barton M, *et al*. Fabrication and Application of Rose Bengal-chitosan Films in Laser Tissue Repair. J Vis Exp 2012:e4158.
[19] Lauto A, Mawad D, Barton M, *et al*. Photochemical tissue bonding with chitosan adhesive films. Biomed Eng Online 2010;9:1–11.
[20] Barton MJ, Morley JW, Mahns DA, *et al*. Tissue repair strength using chitosan adhesives with different physical-chemical characteristics. J Biophotonics 2014;8:1–8.
[21] Glass P, Chung H, Washburn NR, Sitti M. Enhanced wet adhesion and shear of elastomeric micro-fiber arrays with mushroom tip geometry and a photopolymerized p(DMA-co-MEA) tip coating. Langmuir 2010;26:17357–62.
[22] Glass P, Chung H, Washburn NR, Sitti M. Enhanced reversible adhesion of dopamine methacrylamide-coated elastomer microfibrillar structures under wet conditions. Langmuir 2009;25:6607–12.
[23] Fernandez JG, Mills CA, Samitier J. Complex microstructured 3D surfaces using chitosan biopolymer. Small 2009;5: 614–20.